Journal of Power Sources 255 (2014) 29–36

Contents lists available at ScienceDirect

Journal of Power Sources

journal homepage: www.elsevier.com/locate/jpowsour

An experimental study of lithium ion battery thermal management using flexible hydrogel films

Rui Zhao [a], Sijie Zhang [a], Junjie Gu [a], Jie Liu [a,*], Steve Carkner [b], Eric Lanoue [b]

[a] Department of Mechanical and Aerospace Engineering, Carleton University, 1125 Colonel By Drive, Ottawa, ON K1S 5B6, Canada
[b] Panacis Inc., 15 Greenfell Crescent, Suite 205, Ottawa, ON K2G 0G3, Canada

HIGHLIGHTS

- A flexible hydrogel based battery thermal management (BTM) system is developed.
- The performance of the proposed system is compared with conventional BTM systems.
- Hydrogel BTM system efficiently controls the temperature rise in discharge tests.
- The proposed system can arrest or postpone battery thermal runaway in nail tests.
- The hydrogel BTM system is of low-cost, space-saving, and contour-adaptable.

ARTICLE INFO

Article history:
Received 13 September 2013
Received in revised form
19 December 2013
Accepted 31 December 2013
Available online 9 January 2014

Keywords:
Lithium ion battery
Battery thermal management
Flexible hydrogel
Sodium polyacrylate
Passive cooling
Nail penetration

ABSTRACT

Many portable devices such as soldier carrying devices are powered by low-weight but high-capacity lithium ion (Li-ion) batteries. An effective battery thermal management (BTM) system is required to keep the batteries operating within a desirable temperature range with minimal variations, and thus to guarantee their high efficiency, long lifetime and great safety. However, the rigorous constraints imposed by the budgets in weight and volume for this specific application eliminate the possible consideration of many existing classical cooling approaches and make the development of BTM system very challenging in this field. In this paper, a flexible hydrogel-based BTM system is developed to address this challenge. The proposed BTM system is based on cost-effective sodium polyacrylate and can be arbitrarily shaped and conveniently packed to accommodate any Li-ion stacks. This BTM system is tested through a series of high-intensity discharge and abnormal heat release processes, and its performance is compared with three classical BTM systems. The test results demonstrate that the proposed low-cost, space-saving, and contour-adaptable BTM system is a very economic and efficient approach in handling the thermal surge of Li-ion batteries.

1. Introduction

Lithium ion (Li-ion) batteries have emerged as the most promising energy storage technology in recent years due to their higher energy density, lighter weight, no memory effect, and lower self-discharge rate, when compared to other rechargeable battery technologies [1]. Although offering many advantages and benefits, the rigorous requirement for the compactness of Li-ion battery packs in many critical applications (e.g., aerospace and military) usually makes it difficult for the implementation of classical battery thermal management (BTM) systems and often gives rise to some safety issues such as overheating or thermal runaway [2]. Even in safe operation, any increase in temperature may significantly shorten the lifecycles of batteries [3–7]. Therefore, a compact and robust BTM system is critically needed to minimize the temperature rise of Li-ion batteries.

In general, a BTM system can be implemented using either an active cooling system or a passive cooling system. The active cooling system is typically achieved by using fans or pumps to circulate coolants (air [8–10], liquid [11], or CO_2 [12,13], etc.) so that the heat can be extracted from the battery packs. For example in Refs. [14,15], the temperature distribution in battery packs was modified by the forced air convection. The batteries with various types of cell arrangements were designed and the energy consumption was formulated as a function of the pressure drop between the inlet and outlet, from which the optimized arrangements of cells and air flow rates can be obtained. Also the study in Ref. [16] demonstrated the effectiveness of water–

* Corresponding author. Tel.: +1 613 520 2600x8257; fax: +1 613 520 5715.
E-mail address: jliu@mae.carleton.ca (J. Liu).

0378-7753/$ – see front matter © 2014 Elsevier B.V. All rights reserved.
http://dx.doi.org/10.1016/j.jpowsour.2013.12.138

ethylene glycol mixture in controlling the temperature of battery pack through the implementation of a constant temperature bath. The spatial and temporal temperature variations during the course of discharge were maintained within 0.5 °C, but the mobility of the liquid used as coolant may cause safety issues, such as the short circuit, in practice. Generally, a reasonable cell arrangement, a well-designed circulation system, and a powerful cooling material are essential in an active cooling system; however, these elements may also make the system much bulky and power-demanding, which restricts its application in portable battery packs (e.g., soldier-worn battery packs). The passive cooling system makes good use of the physical properties of various coolants implemented between neighboring battery cells to absorb the heat released during the operation, thereby keeping the battery temperature at a relatively low level. The present passive cooling systems usually rely on phase change materials (PCM) for heat absorption. Al Hallaj has first introduced the PCM to thermal management system for the 18650 battery pack [17]. In his study, the temperature of cells and the temperature distribution across the battery pack were inspected at various depths of discharge, and the comparison with air cooling showed the effectiveness of PCM in battery temperature control. However, the PCM material based passive thermal management system often suffers from the following three inherent limitations: 1) high melting point of the PCMs. The relevant battery cells need to reach the melting points (typically higher than 40 °C) of PCMs to utilize their phase change properties. Such high temperature will shorten the life span of the battery; 2) low specific heat capacity of the PCMs (both solid state and liquid state). This will lead to the dramatic rise in the temperature of the battery pack when the PCM temperature is below the melting range; and 3) poor thermal conductivity of the PCMs. This often results in slow heat dissipation and uneven heat distribution, which is extremely harmful to the health of the battery pack and may even lead to an explosion [18,19]. Although various strategies for PCM matrix optimization based on the PCM/graphite mixture have been reported in recent years [20,21], which can provide higher thermal conductivity, but the specific heat capacity of the PCM matrix will in turn be significantly reduced (below 2 kJ kg^{-1} K^{-1}) when inserted into the graphite. Moreover, the preparation of the PCM/graphite matrix is usually a time-consuming and costly process.

To develop a novel passive cooling system to overcome the limitations associated with the classical PCMs, a flexible hydrogel-based BTM system is proposed in this paper. The proposed system is based on sodium polyacrylate (PAAS) hydrogel, which possesses the following advantages: 1) low cost and high flexibility. PAAS is a type of polymer that has been widely used in daily life for liquid absorption (e.g., diapers). The PAAS-based hydrogel is usually of low cost and can be flexibly packed to accommodate any shapes of battery packs; 2) strong water absorbing capacity. Owing to a great number of hydrophilic groups in the three-dimensional chemical chains, the PAAS polymer has the ability to absorb as much as hundreds of times its mass in water. On one hand, the absorbed water is superior in heat control thanks to its high sensible heat; and on the other, the mobility of water can be well managed in operation; and 3) simple and controllable manufacturing process. The proposed BTM system has been validated through a series of experimental tests: first, the battery packs with two different capacities were tested under normal operations at various discharge currents; second, penetration tests were performed on the charged batteries. The performance of the proposed BTM system is compared with three conventional BTM systems (an active air-cooling system, a passive PCM cooling system, and a natural convection system). The testing results demonstrate that the proposed hydrogel-based BTM system is more effective than the other BTM systems in keeping battery packs' temperature stable within an allowable range in discharge tests and preventing the occurrence of thermal runaway in penetration tests.

Table 1
Specifications of two battery packs.

	Pack 1	Pack 2
Pack operating voltage	3.0–4.2 V $cell^{-1}$ (6–8.4 V $pack^{-1}$)	3.0–4.2 V $cell^{-1}$ (15–21 V $pack^{-1}$)
Pack capacity	1300 mAh	8000 mAh
Total weight of pack		
Ambient	58.7 g	926.75 g
Hydrogel	70.6 g	1178.02 g
PCM	68.66 g	1146.24 g
Cooling fan	240.32 g	1108.37 g
Spacing between cells	2 mm	4.5 mm
Discharge rate	1C, 2C, 4C	1C

2. Experimental

2.1. Constant current discharge tests

Two 1300 mAh and five 8000 mAh pouch Li-ion cells were selected to construct two battery packs in the constant current discharge tests, in which the cells were connected in series and the space between neighboring cells were half the thickness of the cell. Table 1 lists the specifications of two battery packs. Four BTM systems (i.e., PAAS hydrogel, traditional PCM (paraffin wax), air-cooling, and natural convection) were built for the cell packs. The tests were performed in cardboard boxes with a dimension of 29.5 cm × 11.5 cm × 11.5 cm in length, width, and height, respectively, to simulate the real circumstances in military backpack, and every battery pack was placed at the center of each box.

Hydrogel BTM system was obtained by injecting deionized water into the pack on the bottom of which polyacrylate sodium (PAAS) particles were evenly distributed. The content of PAAS is 1 wt.%. Fig. 1 shows the 8000 mAh battery pack with hydrogel coolant embedded in. The specific capacity and heat conductivity of the hydrogel are expressed as follows:

$$Cp_{gel} = \varepsilon Cp_{PAAS} + (1-\varepsilon)Cp_{H_2O}, \quad (1)$$

$$k_{gel} = \varepsilon k_{PAAS} + (1-\varepsilon)k_{H_2O}, \quad (2)$$

where Cp is the specific heat capacity, k is the heat conductivity, and ε is mass content of PAAS particles. As for the PCM cooling system, the battery cells were inserted into the matrix prepared in advance. The air-cooling thermal management was achieved by placing a cooling fan of 8 cm × 8 cm at one side of the battery pack with a distance of 5 cm, and the rotation speed of the fan was set at 1500 rpm.

Before loading, both battery packs were charged at a specific C-rate with the voltage cut-off limits of 8.4 V and 21 V (4.2 V for each cell), respectively, followed by a potentiostatic mode until the current drops to 0.02C. It took 1 h for the battery cells to equilibrate, and then the discharge tests were carried out at different C-rates until the voltage drops to 3 V per cell. In the discharge process, a thermistor was attached at the center of the battery pack (i.e., the position more susceptible to overheating) to measure the temperature variation. The initial temperature inside the test cardboard boxes was kept at 23 °C.

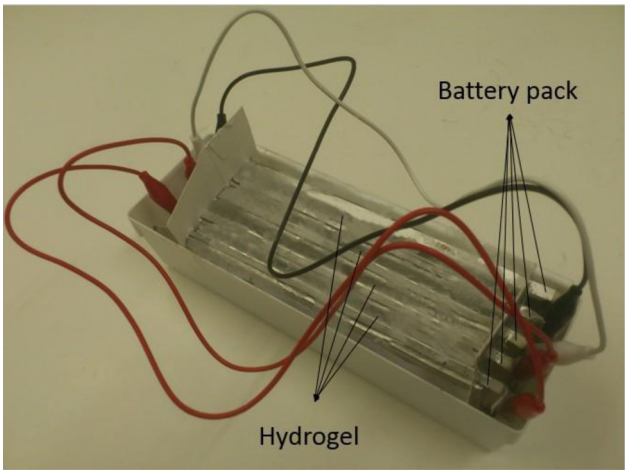

Fig. 1. Hydrogel thermal management system on 8000 mAh battery pack.

2.2. Penetration tests

Penetration tests were conducted on 8000 mAh cells. The cells were preconditioned under constant current of 0.1C between 3.0 V and 4.2 V, and finished at charged state prior to the tests. Each charged sample cell was then encased in a container of 20 cm × 6.5 cm × 5.5 cm. Depending on the thickness of the coolants used in the container, the testing systems were divided into "heavy system (HS)" and "light system (LS)" as schematically shown in Fig. 2a and b. The small blocks in the figures represent the wood brackets which are able to secure the cells during the tests. The PCM, water and hydrogel were employed as coolants during tests, and the thickness of the coolants on either side of the cell was 2 cm and 1 cm in HS and LS, respectively. For accuracy, totally three cells were penetrated for each testing system, and the ambient temperature was 15 °C during the tests.

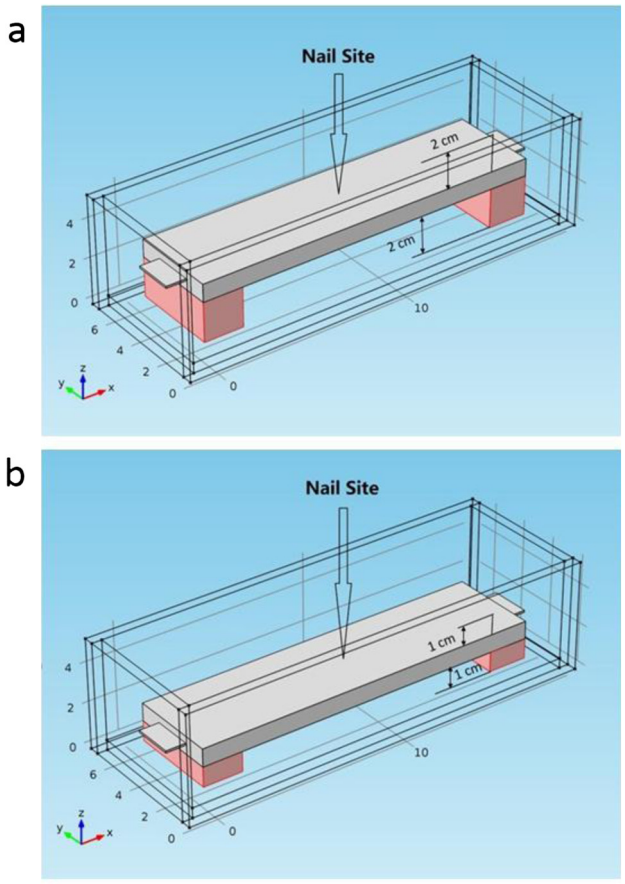

Fig. 2. Schematic illustration of two penetration systems: (a) heavy system and (b) light system.

Table 2
List of information on experimental groups.

Test number	Battery size (cm^3)	Nail type	Protection system	HS or LS
1		2	Ambient	HS
2		1	Ambient	HS
3	17.5 × 4.5 × 0.9	2	PCM	HS
4		2	Water	HS
5		2	Hydrogel	HS
6		2	Hydrogel	LS

Based on the nail types and coolants, six groups of tests were carried out in either the HS or LS, which are summarized in Table 2. The nail type 1 and 2 represent the hardwood ($R > 60$ MΩ) and steel ($R = 0.2$ Ω) nail of 3-mm diameter, respectively. During each test, the penetrating process was performed and then followed by a retracting procedure, both of which have a velocity of 5 cm s^{-1}. In addition, a digital voltmeter and an infrared thermometer were employed during the tests to measure the voltages and temperatures of the cells, respectively.

3. Results and discussion

3.1. Control of temperature rise

The heat dissipation capacities of these four BTM systems were evaluated by comparing: a) the temperature rises of the 1300 mAh Li-ion battery packs at three discharge rates (i.e., 1C, 2C, and 4C); and b) the temperature rises of the 8000 mAh battery pack at the discharge rate of 1C. The testing results are summarized in Table 3 and in the meantime Figs. 3 and 4 respectively show the detailed temperature vs. time profiles of the 1300 mAh and 8000 mAh battery packs with four BTM strategies during the discharge processes, from which the following observations can be made: 1) the PAAS hydrogel performs similarly as the cooling fan does when dealing with low-capacity battery packs at low discharge rates (e.g., 1C and 2C); 2) both the PAAS hydrogel and the cooling fan perform much better than the other two BTM systems in suppressing the temperature rises when dealing with low-capacity battery pack at low discharge rates; and 3) the PAAS hydrogel demonstrates its superiority over the other three BTM systems in controlling the temperature rises when dealing with high-capacity battery packs or when dealing with low-capacity battery packs but at high discharge rates (e.g., 4C).

Table 3
Summary of the temperature rises at the center of battery modules during the discharge cycle at various C-rates in different BTM systems.

Discharge current	Ambient (°C)	Cooling fan (°C)	Traditional PCM (°C)	PAAS hydrogel (°C)
1.3 A (1C)[a]	4.3	2.7	3.3	2.9
2.6 A (2C)[a]	10.7	4.8	6.7	5.6
5.2 A (4C)[a]	16.7	8.6	11.5	7.5
8 A (1C)[b]	16.3	11.8	10.9	6.7

[a] 1300 mAh battery pack.
[b] 8000 mAh battery pack.

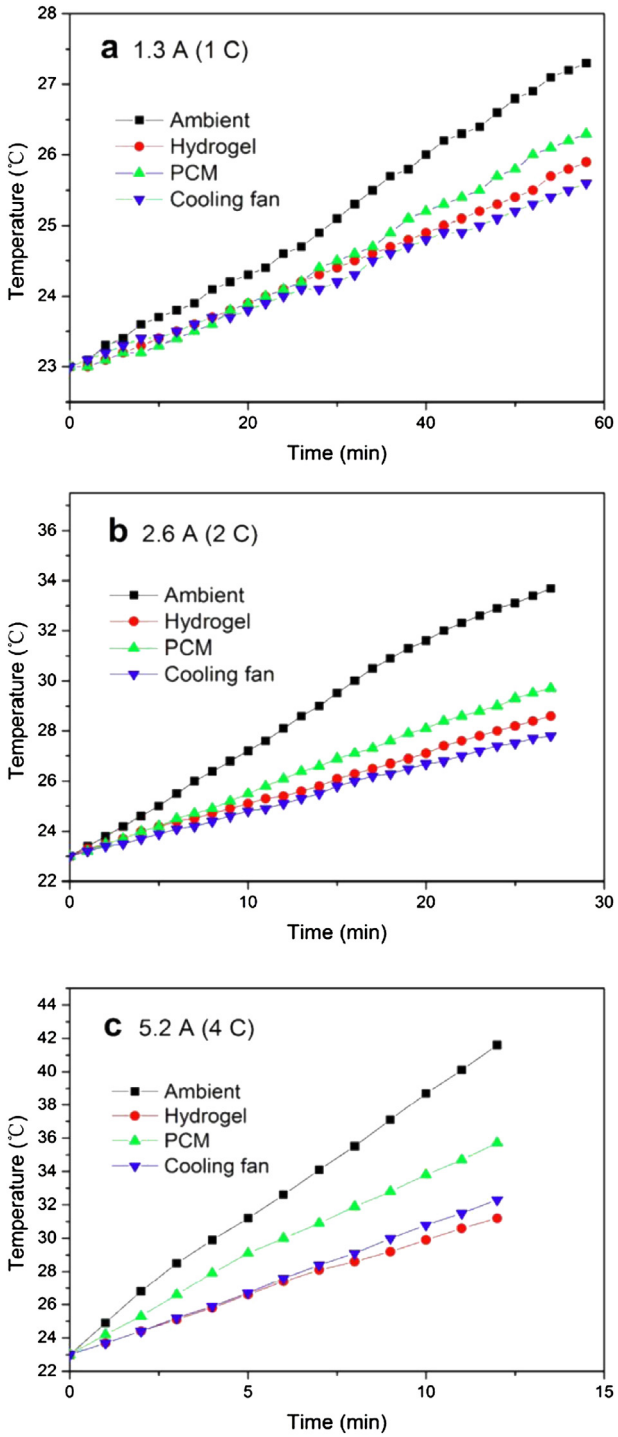

Fig. 3. Temperature vs. time profiles of 1300 mAh battery pack with four BTM strategies in the discharge processes at discharge rates of (a) 1C, (b) 2C, and (c) 4C.

After validating the effectiveness of the hydrogel cooling system in controlling the temperature rise during discharge, the feasibility of implementing it in real applications needs to be verified. Generally, a qualified passive BTM system requires the cooling material filled inside remains stable over the whole temperature range of battery usage. Since water is known to be evaporating and changing volume during phase change (from liquid to solid at low temperatures), the consequent mass decrease and volume change of hydrogel and the relevant safety issues caused by moisture

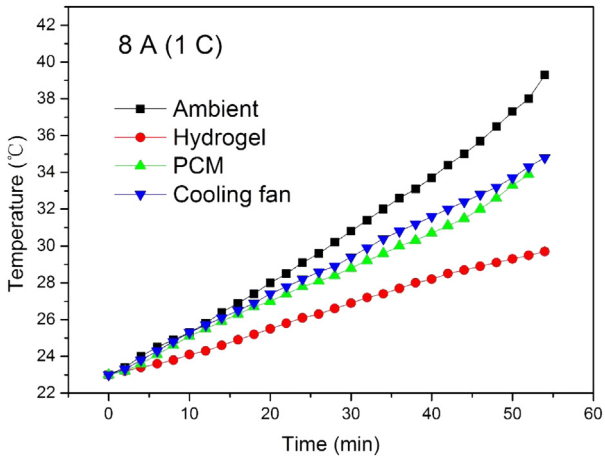

Fig. 4. Temperature vs. time profile of 8000 mAh battery pack with four BTM strategies in the discharge processes at a discharge rate of 1C.

deserve further investigation. First, an evaporation test has been carried out by placing two 25 ml graduated cylinders, filled with water and hydrogel, respectively, in the environmental chamber at 80 °C for 12 h, and the testing results show that the average evaporation rates for water and hydrogel are 0.46 and 0.38 g h^{-1}, respectively, under this testing condition. The relatively lower evaporation rate for hydrogel is attributed to the hydrogen bonds between PAAS and water, and it requires more energy for the water to vaporize out from the networks. To better address this water evaporation issue, the methods based on an open structure and a closed structure are proposed for future applications. In an open structure, the hydrogel system wrapped around the battery pack is designed with a refilling inlet and a venting outlet. The inlet facilities the BTM system to be refilled with water periodically while the outlet allows the vapor to be evaporated directly to the ambient, thereby hindering the rise of humidity around the battery tabs and alleviating the relevant safety concerns. In practice, the application of the open structure needs to take into consideration with several important factors such as the hydrogel amount monitoring, the opening size, and the refilling frequency. The complexity involved in designing such an open structure makes it more suitable for the large and stationary battery systems, where a fully automated online supervision system can be implemented. As for the small-scale and/or mobile applications, a closed structure rather than an open one is more preferred. As the name implies, in a closed structure, the battery package with hydrogel BTM system is completely sealed with only the battery tabs left outside. Since the saturated pressure of water is as low as 47.39 kPa, which is less than half the atmosphere pressure, even at 80 °C (when the vapor and water coexist) [22], the sealed battery pack is safe and stable at high temperatures and there would be no mass loss and humidity increase. Second, the volume changes of water and PAAS hydrogel are further investigated. Although the water expands (by approximately 8.3%) from liquid state to solid state, the volume change of hydrogel

Table 4
Thermal properties of PAAS hydrogel and PCM used as BTM materials in the discharge tests.

Thermal property	PCM	PAAS hydrogel
Specific heat capacity (kJ kg^{-1} K^{-1})	2.14	4.18
Thermal conductivity (W m^{-1} K^{-1})	0.25 (solid) 0.19 (liquid)	0.58
Melting range (°C)	42–45	–

during phase change is much smaller (only 3.47%). This is due to the already-experienced expansion of hydrogel during gelatinization. Also, the density of hydrogel at room temperature (23 °C), around 950 kg m^{-3}, is close to the lowest ice density (at 0 °C), 917 kg m^{-3}. The small volume expansion caused by the difference in density can be readily resolved by leaving a small void space inside the pack. This approach has been successfully applied to the PCM-based (phase change expansion of 15%) BTM system [23–25]. Also to avoid expansion, a certain amount of ethylene glycol can be added to water prior to the gel reaction, considering the low temperature level. In Ref. [16], a temperature bath based on this mixture has been applied to control the battery temperature, and the mixture has been proved to be functioning at −20 °C in liquid state. Our recent low temperature test also shows that the PAAS hydrogel mixed with 35 wt.% ethylene glycol is ice-free down to −20 °C. It should be noted that in extremely cold conditions a heating system rather than a cooling one may be used.

3.2. Detailed comparison of the BTM systems

For battery packs, the heat generated can be expressed as:

$$Q = I^2R - IT\frac{dV_{oc}}{dT}, \quad (3)$$

where Q is the heat generated, I is the current, R is the resistance of the battery pack, T is temperature and V_{OC} is the open circuit voltage of battery pack. The first term on the right hand side of the above equation is the heat generated due to the ohmic resistance, and the second term refers to the reversible heat due to the entropy change of electro-chemical reactions. The discharge occurs when $I > 0$ and the term dV_{OC}/dT is always negative. As a result, the second term on the right hand side of the above equation is positive during discharges [26]. With this in mind, the comparison of the performances of these BTM strategies in suppressing the battery pack thermal surge is elaborated in the following context.

3.2.1. PAAS hydrogel vs. active air-cooling

Both the PAAS hydrogel and the air-cooling method prove to be very effective in controlling the temperature rises of the battery packs during the low current discharge processes. For the 1300 mAh battery packs, the air-cooling BTM system performs better but consumes a certain amount of power that cannot be neglected. For example, the power consumed by the cooling fan in 1C discharge process of the 1300 mAh battery pack accounts for as much as 30% of the total energy of the pack. This would impose challenges to portable battery packs in real-world applications. At high current discharge tests, although the percentage of the power consumed by fan is reduced, the performance of cooling fan BTM system shows to be less effective than the hydrogel system (Fig. 4). This is because more heat is generated when the current increases based on Eq. (3), however, the heat dissipation rate of cooling fan remains unchanged. By contrast, the hydrogel-based BTM system has a passive cooling mechanism, and the quantity of hydrogel is varied with the size of the cell without compromising the compactness of the whole battery pack, which ensures its effectiveness in controlling the thermal surge when dealing with various battery packs.

3.2.2. PAAS hydrogel vs. traditional PCMs

The PAAS hydrogel and traditional PCMs are used as passive cooling methods in the discharge tests and their thermal properties are listed in Table 4. Given that 99 wt.% of water is contained in the hydrogel, the specific heat capacity and heat conductivity of the hydrogel can be determined by its water content. In all the discharge tests, the proposed PAAS hydrogel outperforms the PCM in controlling the temperature rises, and the superiority of the PAAS hydrogel over the PCM becomes more evident when dealing with higher capacity battery packs or discharging at high rates. This is because: 1) from the specific heat capacity perspective, the PCM can generally absorb a great amount of heat without a marked temperature change in the phase change process. However, this phase change process usually takes place at a relatively high temperature range (42–45 °C in our case), which may already adversely affected the health of the battery packs (it is reported that the life span of Li-ion batteries can be reduced by about two months for every degree of temperature rise in an operating range of 30–40 °C [27]). The ideal operational temperature range for Li-ion batteries is usually around 30 °C that is still under the melting points of the most traditional PCMs, where the sensible heat rather than the latent heat is the major source of the absorbed heat. Given that the PAAS hydrogel typically possesses twice the specific heat capacity of the PCMs, the hydrogel based BTM system can perform much better than the PCMs in suppressing the battery pack temperature rises within this temperature range. 2) From the heat conductivity perspective, the heat conductivity of the PAAS hydrogel is approximately 0.58 W m^{-1} K^{-1} at 25 °C, much higher than those of most PCMs (approximately 0.25 W m^{-1} K^{-1} at 25 °C), and their heat conductivities increase almost linearly as the temperature rises. Owing to its higher heat conductivity, the hydrogel based BTM system is capable of distributing the heat in a more efficient manner, especially when dealing with high-capacity battery pack discharge or discharge at high rates.

3.3. Prevention of thermal runaway

In this experimental study, a series of penetration tests have been conducted to verify the capability of the proposed PAAS hydrogel based BTM system in handling an extreme condition (i.e., battery thermal runaway) that may occur in real-world applications. In the first round, four groups of tests were carried out. Test Group #1 and #2 were designed to compare the level of risks that may be incurred by two types of nails, hardwood nails and steel nails that respectively represent insulating penetrators and conducting penetrators. These two groups of tests were performed at an ambient temperature (15 °C). The tests revealed that the involved cells bulged with an intensive venting and the surface temperature experienced a dramatic increase and exceeded 500 °C. As an example, a popped cell penetrated by a wood nail is shown in Fig. 5. Unpacking the damaged cells, the deformations around the

Fig. 5. Photograph of a seriously damaged cell penetrated by a wooden nail.

Table 5
Summary of Li-ion battery testing results in test 1–4.

Test no.	Voltage before penetration (V)	Voltage after penetration (V)	No. of cells tested	Maximum surface temperature (°C)	No. of cells vented
1	4.15	0	3	>350	3
2	4.15	0	3	>500	3
3	4.15	0	3	>450	3
4	4.15	0	3	<150	3

Table 6
Penetration results for the cells tested in the hydrogel thermal management system.

Test no. & cell no.		Penetrated hole(s)	Venting or not	Response time (s)	Voltage before penetration test (V)	Voltage after first penetration (V)	Voltage after second penetration (V)
5	1	1	No	–	4.15	4.09	–
	2	2	No	–	4.15	4.09	4.02
	3	3	Yes[a]	3	4.15	4.08	4.01
6	1	1	No	–	4.15	4.09	–
	2	1	Yes	150	4.15	–	–
	3	2	Yes	60	4.15	4.08	–

[a] Venting takes place at the third penetration without the protection of hydrogel thermal management system.

penetrated holes were observed, and also the anodes were found in touch with the adjacent cathodes, which caused serious internal short-circuits (ISCr). It is believed that the large current caused by ISCr led to a dramatic temperature rise, which in turn initiated the thermo-chemical chain reactions of the electrolyte, electrodes, and separators within each battery cell, thereby generating a huge amount of heat [28,29]. It was also observed that the response time (i.e., the time interval between nailing and cell popping) caused by steel nails was about 2 s that is much shorter than the 10 s response time caused by wood nails due to the relatively much higher electric conductivity of the steel. As such, more testing has been done in the following experiments (i.e., Group Tests #3–#6) with the steel nailing to compare the performance of the PAAS hydrogel and PCM in suppressing battery thermal runaway.

The traditional PCM was employed in Group Test #3 for handling the battery thermal runaway, where the test cells were fastened at the center of the container with 2 cm PCM stacked on both sides (i.e., the HS as shown in Fig. 2a). When the cells were penetrated, they immediately experienced a severe thermal runaway. The intensive venting and the sudden deformation of the cells pushed the top layer of PCM out of the container. The surface temperatures of the cells were measured to be over 450 °C. Meanwhile, the bottom layer of PCM melted down as a result of the high temperature and huge heat accumulation. It is experimentally found that the traditional PCM is not effective in preventing the battery thermal runaway in this battery penetration test.

Considering water is the major component (in terms of wt.%) of the proposed PAAS hydrogel based BTM system, Group Test #4 only applies water in the HS to evaluate its viability in preventing the occurrence of thermal runaway. In this testing, the positive and negative electrodes of the cells were sealed before immersing them into the water. Immediately after the nails were retracted from the cells, bubbles were continuously generated from the nailed hole at an increasing speed. In about 5–10 s, white smoke were generated from the test cells and the cells then severely vented and popped, as similarly seen from the penetration tests in ambient conditions. However, the surface temperatures of the test cells remain below 150 °C, compared to over 500 °C in the ambient testing case. The testing results from the Group Test #1–#4 are summarized in Table 5.

The testing results from the Group Test # 3 (PCM) and #4 (water) will serve as the benchmarks for the subsequent testing in Group Test #5 (PAAS hydrogel in HS) and #6 (PAAS hydrogel in LS) to verify the effectiveness of the proposed hydrogel based BTM system in battery thermal runaway suppression. In Group Test #5, the PAAS hydrogel (1 wt.%) was injected into the HS as the thermal management material. In contrast to the severe reactions that occurred in Group Test #4 (water), all of the tested three cells in Group Test #5 (immerged in hydrogel) passed the penetration testing without incurring thermal runaway (even no venting). Table 6 summarizes the testing results. As an example, Fig. 6 shows one cell with two nailing holes. After penetration, the voltages of two cells dropped to 0 V after 12 h. For further performance validation, a third nailing is performed on the third tested cell in which the hydrogel has been completed dumped; the cell quickly went to venting. These testing results demonstrate the effectiveness of the proposed PAAS hydrogel in maintaining the stability of the Li-ion battery cells under nail penetration. To physically understand this finding, Fig. 7 represents the motion of ions and electrons between adjacent electrodes when the cell is nailed. With the separator as the barrier, the electrons can only migrate in the nailing region, which leads to a higher current density, and more heat will then be generated locally. If the excessive thermal heat cannot be dissipated

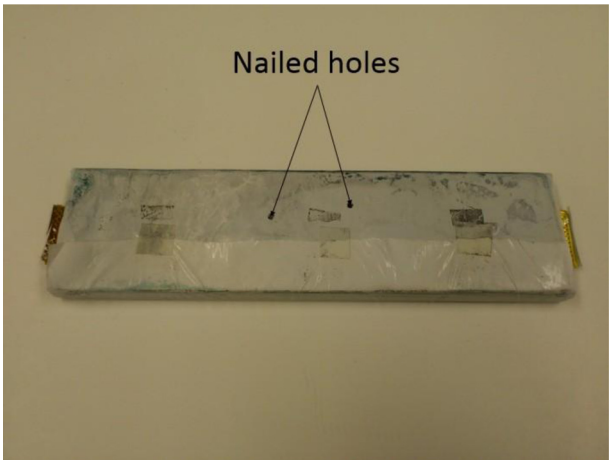

Fig. 6. Photograph of a sample cell penetrated in hydrogel BTM system.

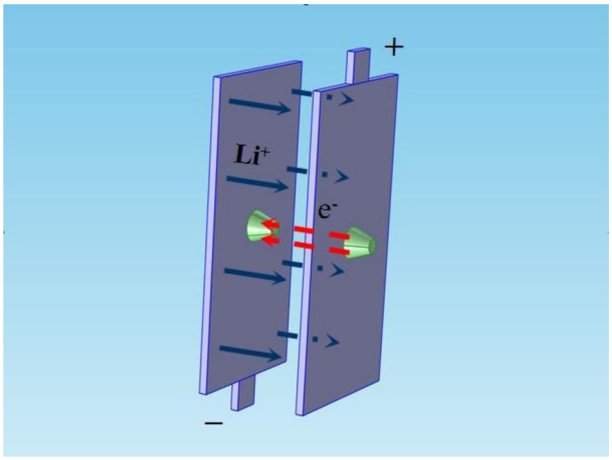

Fig. 7. Schematic diagram of the motion of ions and electrons in adjacent electrodes after penetration.

efficiently, the dramatic temperature rise will cause the separators around the nailing holes to shrink, thereby leading to more severe ISCr. Both the hydrogel and water have the capability to cool down the cells, but the difference in their viscosities can lead to significantly different performances. After the cells being penetrated, a certain amount of fumes are generated due to internal thermo-chemical reactions, which creates a high pressure inside the nailing hole that in turn blows the coolant (either hydrogel or water) out. Due to its much lower viscosity, water is more susceptible to be blown away, and this is the reason why the temperature in the nailing region of the water based HS increases dramatically in the cell penetration tests. Furthermore, the electrical resistance of hydrogel is usually 15 times of that of water with electrodes immersed, which leads to much less heat generation under the same ISCr circumstance.

For comparison with the testing results (HS) from Group Test #5, Group Test #6 applies hydrogel in the LS setting. As summarized in Table 6, three cells were tested. Among them, one cell did not vent and its voltage gradually dropped to 0 V after 12 h. The other two cells went on venting with the response time to be 150 s and 60 s, respectively. The testing results indicate that a lower amount of hydrogel will correspondingly reduce the level of protection in battery thermal runaway. This is because the less hydrogel provides a lower pressure on the battery surface that is insufficient to balance the pressure generated inside the nailing hole caused by the cell internal chemical reaction. Moreover, when the cell is nailed, a longer time is required for the hydrogel in LS to enter the nailed holes to insulate the electrodes and control the temperature rise, so the increased temperature may still be able to initiate some internal reactions.

4. Conclusions

A study on implementing a novel hydrogel based system for Li-ion battery thermal management (BTM) was carried out in this work. The effectiveness of the hydrogel based BTM in heat dissipation is validated in both the constant current discharge processes and the nail penetration tests. Based on the high moisture content, the hydrogel based BTM keeps the most advantages of water (i.e., high specific heat capacity and medium heat conductivity) and in the meantime the mobility of water is prevented. In discharge tests, the proposed hydrogel BTM system shows its effectiveness in dissipating the generated heat from the battery packs without requiring an additional power supply. The advantage of hydrogel BTM systems in dealing with extreme conditions is also tested through a series of nail penetration tests. Relying on its high resistance, high viscosity and high specific heat capacity, the proposed hydrogel based BTM system can either extend the safety time or prevent the occurrence of thermal runaway, and the voltages of the battery cells after the penetration testing can still remain at a high level.

As a final note, the proposed hydrogel based BTM system is targeted to stationary or mobile battery packs that require a compact, accessible, and power-saving cooling system to suppress the unexpected thermal surge or runaway under normal and extreme conditions. This BTM system can be implemented in an open or a closed structure to address the problems associated with evaporation, humidity and volume change during phase change, and the packaging of the proposed cooling system can be customized based on the size and shape of the electric device. Meanwhile, a PAAS hydrogel consisting of the water–ethylene glycol mixture would be suggested to prevent the hydrogel from icing at sub-zero temperatures.

Acknowledgments

This project is financially supported by Natural Sciences and Engineering Research Council (NSERC) of Canada and Panacis Inc. located in Ottawa, Ontario. The authors would like to acknowledge the help of Dr. Zhonghua Zhang for his assistance in the preparation of this manuscript. The valuable comments and suggestions from the anonymous reviewers would also be much appreciated.

References

[1] V. Etcheri, R. Marom, R. Elazari, G. Salitra, D. Aurbach, Energy Environ. Sci. 4 (2011) 3243–3262.
[2] http://www.eere.energy.gov/vehiclesandfuels/pdfs/program/fc_fuel_partnership_plan.pdf, (accessed 12.07.10).
[3] C. Park, A.K. Jaura, Reciprocating Battery Cooling for Hybrid and Fuel Cell Vehicles, IMECE 2003-41201.
[4] C. Park, A.K. Jaura, Transient Heat Transfer of 42 V Ni-MH Batteries for an HEV Application, SAE 2002-01-1964.
[5] J. Wang, P. Liu, J. Hicks-Garner, E. Sherman, S. Soukiazian, M. Verbrugge, H. Tataria, J. Musser, P. Finamore, J. Power Sources 196 (2011) 3942–3948.
[6] C. Park, A.K. Jaura, Dynamic Thermal Model of Li-Ion Battery for Predictive Behavior in Hybrid and Fuel Cell Vehicles, SAE 2003-01-2286.
[7] R.B. Wright, J.P. Christophersen, C.G. Motloch, J.R. Belt, C.D. Ho, V.S. Battaglia, J.A. Barnes, T.Q. Duong, R.A. Sutula, J. Power Sources 119–121 (2003) 865–869.
[8] X.M. Xu, R. He, J. Power Sources 240 (2013) 33–41.
[9] M.R. Giuliano, A.K. Prasad, S.G. Advani, J. Power Sources 216 (2012) 345–352.
[10] Z. Zhang, L. Jia, N. Zhao, L. Yang, J. Therm. Sci. 20 (2011) 570–575.
[11] G. Eggen, G. Vangsnes, in: The 8th IEA Heat Pump Conference, 2005.
[12] S.C. Kim, J.P. Won, Y.S. Park, T.W. Lim, M.S. Kim, Int. J. Refrig. 32 (2009) 70–77.
[13] D.Y. Leea, C.W. Chob, J.P. Wonb, Y.C. Parkc, M.Y. Lee, Appl. Therm. Eng. 50 (2013) 660–669.
[14] H. Park, J. Power Sources 239 (2013) 30–36.
[15] L. Fan, J.M. Khodadadi, A. Pesaran, J. Power Sources 238 (2013) 301–312.
[16] K. Chen, X. Li, J. Power Sources 247 (2014) 961–966.
[17] S. Al-Hallaj, J.R. Selman, J. Electrochem. Soc. 147 (2000) 3231–3236.
[18] A. Pesaran, J. Power Sources 110 (2002) 377–382.
[19] P. Ramadass, B. Haran, R. White, B.N. Popov, J. Power Sources 112 (2002) 614–620.
[20] R. Kizilela, R. Sabbaha, J.R. Selmana, S. Al-Hallaj, J. Power Sources 194 (2009) 1105–1112.
[21] S.G. Jeong, O. Chung, S. Yu, S. Kim, S. Kim, Sol. Energy Mater. Sol. Cells 117 (2013) 87–92.
[22] M.J. Moran, H.N. Shapiro, D.D. Boettner, M.B. Bailey, Fundamentals of Engineering Thermodynamics, seventh ed., John Wiley & Sons, Inc, New York, 2011.
[23] http://www.google.ca/url?sa=t&rct=j&q=&esrc=s&source=web&cd=3&ved=0CEIQFjAC&url=http%3A%2F%2Fwww.electrochem.org%2Fdl%2Fma%2F200%2Fpdfs%2F0305.pdf&;ei=bTerUvGcC8q0rgGupYHABQ&usg=AFQjCNH1TpihQYIv4ngFXHRveBusbtvu8w&sig2=w537PT59kcs78axLoFIGjA, (accessed 09.07.13).
[24] J.S. Lee, S. Lucyszyn, Sens. Actuators A Phys. 135 (2007) 731–739.

[25] S.A. Khateeb, S. Amiruddin, M. Farid, J.R. Selman, S. Al-Hallaj, J. Power Sources 142 (2005) 345–353.
[26] M.R. Giuliano, S.G. Advani, A.K. Prasad, J. Power Sources 196 (2011) 6517–6524.
[27] C.G. Motloch, J.P. Christopheresen, J.P. Belt, R.B. Wright, G.L. Hunt, R.A. Sutula, T. Duong, T.J. Tartamella, H.J. Haskins, T.J. Miller, High-Power Battery Testing Procedures and Analytical Methodologies for HEV's, SAE 2002-01-1950.
[28] H. Maleki, J.N. Howard, J. Power Sources 191 (2009) 568–574.
[29] W. Cai, H. Wang, H. Maleki, J. Howard, E.L. Curzio, J. Power Sources 196 (2011) 7779–7783.